Imagerie Médicale : Principes Physiques, traitement Numérique et Applications Avancées

Ecole Centrale Paris (Option Math. App) -

Mastère Recherche MVA - Mastère IDB – 2007/2008

X. Pennec

Tensor computing & Computational Anatomy

INRIA SOPHIA ANTIPOLIS

Asclepios team
2004, route des Lucioles B.P. 93
06902 Sophia Antipolis Cedex

http://www-sop.inria.fr/asclepios

Cours 2e module

Lundi 14 janvier 2008:	Delingette (Rappels 1er module et classification)
Lundi 21 janvier 2008:	Pennec (Recalage paramétrique géométrique)
Lundi 28 janvier 2008:	Pennec (Recalage non rigide iconique)
Lundi 18 fevrier 2008:	Pennec (Tenseurs & anatomie algorithmique)
Lundi 25 fevrier 2008:	Delingette (Modèles biomécaniques)
Lundi 3 mars 2008:	Pennec /Delingette (Quizz et présentation d'articles)
Lundi 10 mars 2008:	Pennec/Delingette (Quizz et présentation d'articles)

Content

Méthodes iconiques : minimisation d'énergie

Critère de similarité + régularisation

$$E(T) \quad = \quad E_{sim}(I, J(T)) \;\; + \;\; \lambda.E_{reg}(T)$$

E_{sim} : **Mesure la ressemblance des intensités entre voxels homologues;**

E_{reg} : **Energie de déformation destinée à régulariser le problème (Thikhonov, modèles d'élasticité linéaire, mécanique des fluides, etc.).**
Bajcsy, Christensen-Miller, Bro-Nielsen, Thirion, Pennec, Cachier, Hellier, Younes, Trouvé, Hermosillo….

- E_{reg} = 0 pour rigide à affine

Pondération intensité / déformation !

Optimal Criterion for Intensity Similarity

Identity: Sum of Square Differences

$$ssd^2 = \sum_k (I(x_k) - J(T(x_k)))^2$$

Affine: Correlation Coefficient

$$\rho^2 = \frac{Cov^2(I, J(T))}{Var(I)}$$

Functional: Correlation Ratio

$$\eta^2 = 1 - \frac{Var(E(I / J(T)))}{Var(I)}$$

Statistical: Mutual Information

$$MI(I,J) = H(I) + H(J) - H(I,J)$$

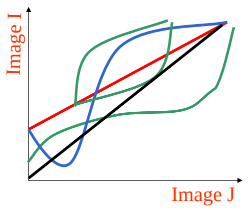

PASHA Algorithm

$$E(C,U) = E_S(I,J,C) + \sigma \int \| C - U \|^2 + \lambda \int \| \nabla U \|^2$$

Adding the correspondences as auxiliary variables:

- Minimization on C by differentiation of the similarity criterion (gradient descent,1st or 2nd order)
- Minimization on U, explicit solution by Gaussian convolution

P. Cachier E. Bardinet, E. Dormont, X. Pennec and N. A.: *Iconic Feature Based Nonrigid Registration: the PASHA Algorithm*, Comp. Vision and Image Understanding (CVIU), Special Issue on Non Rigid Registration, 89 (2-3), 272-298, 2003.

Inter-subject hybrid non-linear registration

PASHA [P. Cathier PhD 2002]

- Demons as an efficient alternated optimization scheme

$$E(C,T) = \mathrm{SIM}(I,J,C) + \tfrac{1}{\sigma^2}\,\mathrm{dist}(C,T)^2 + \mathrm{Reg}(T)$$

- Hybrid iconic and feature-based criteria

[Cachier et al, MICCAI 2001, CVIU 89(2-3), 2001]

Content

Recalage iconique et deformable (rappel)

Imagerie du tenseur de diffusion

Tensor Computing

Computational Anatomy

Conclusion

L'imagerie de diffusion : Introduction

- Technique apparue au milieu des années 80 (Basser, LeBihan).
- IRM classique : image la substance blanche, grise et le liquide céphalorachidien.
- IRM de diffusion : image in vivo l'architecture de la matière blanche.
- Aussi appelée « Imagerie du Tenseur de Diffusion », ou « Diffusion Tensor Imaging » (DTI).

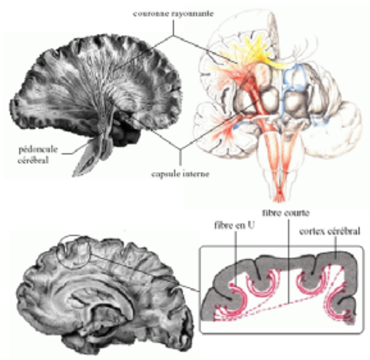

La substance blanche

- Substance blanche = ensemble de fibres nerveuses (axones).
- Comparable aux câbles d'un réseau : ces liaisons relient les zones de traitement (cortex) entre elles.
- Aussi important à contrôler que les zones de traitement elles-mêmes.
- Le phénomène de diffusion permet d'accéder a cette information.

Le phénomène de diffusion

- Mouvement Brownien (Einstein) : les molécules dans un milieu s'entrechoquent et changent de direction sans arrêt.
- Phénomène microscopique : mouvement brownien. Phénomène macroscopique : diffusion.
- Si milieu isotrope : la probabilité de déplacement d'une molécule est la même quelque soit la direction.
- Si milieu anisotrope : la probabilité de diffusion/déplacement dépend de la direction de l'espace => tenseur.

Le Tenseur

Def. mathématique : application multilinéaire (généralisation de l'algèbre linéaire, i.e. des matrices) : On oublie.

Ici : matrices symétriques réelles définies positives.

- Réelles def. positive = valeurs propres toutes réelles et >0.
- Forme quadrique = ellipsoïde.

$$D = \begin{pmatrix} d_{xx} & d_{xy} & d_{xz} \\ d_{xy} & d_{yy} & d_{yz} \\ d_{xz} & d_{xz} & d_{zz} \end{pmatrix}$$

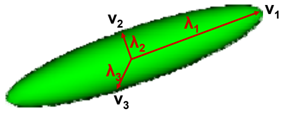

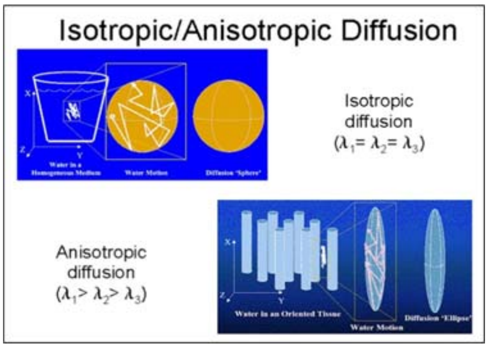

Anatomie d'une séquence IRM de diffusion

Image T2

+

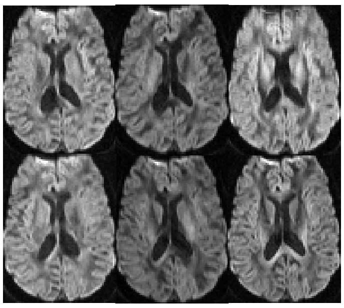

6 images pondérées en diffusion

Équation de Stejskal & Tanner

Atténuation du signal reliée au tenseur par :

$$S_i = S_0 \exp\left(-b \vec{g}_i^T D \vec{g}_i\right)$$

- S_i : image dite pondérée en diffusion;
- S_0 : image T2;
- g_i : direction spatiale du gradient de diffusion;
- b : b-value (relié aux paramètres physiques de l'acquisition);
- D : tenseur de diffusion;

Reconstruction du tenseur de diffusion

- **Tenseur : 6 degrés de liberté.**
  - Au moins 6 images acquises avec 6 gradients non colinéaires.
- **Linéarisation de l'équation de Stejskal & Tanner :**

$$\log\left(\frac{S_0}{S_i}\right) = b \vec{g}_i^T D(x) \vec{g}_i$$

- **Estimation du tenseur aux moindres carrés :**

$$D(x) = \min \sum_{i=1}^{N} \left(\log\left(\frac{S_0}{S_i}\right) - b \vec{g}_i^T D(x) \vec{g}_i\right)^2$$

- **D'autres méthodes possibles :**
  - équations non-linéaires, m-estimateurs.

Coefficients du tenseur

$$\begin{bmatrix} d_{xx} & d_{xy} & d_{xz} \\ & d_{yy} & d_{yz} \\ & & d_{zz} \end{bmatrix}$$

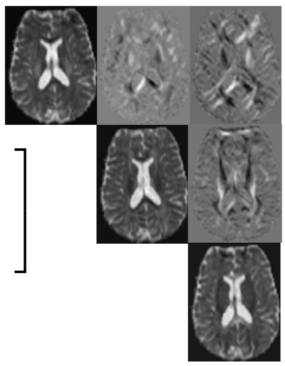

Visualisation par ellipsoïdes

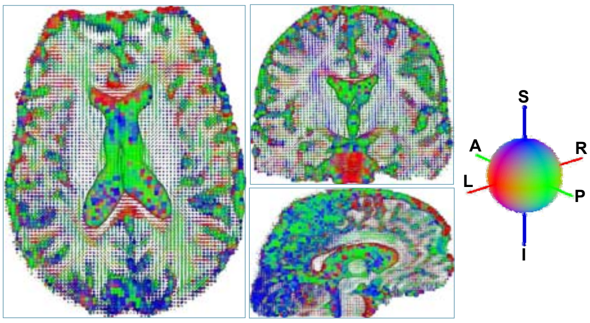

Coefficients dérives du tenseur

- Difficile de visualiser et d'interpréter des images de tenseurs.
- Information riche (direction, amplitude de la diffusion).
- Nécessite de condenser l'information en une image scalaire simple à interpréter pour les cliniciens.

Le Coefficient de Diffusion Apparente

- **Apparent Diffusion Coefficient (ADC) = trace du tenseur :**

$$\mathrm{ADC} = \mathrm{trace(D)} = \sum_{i=1}^{3} \lambda_i$$

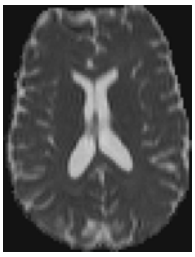

- **Renseigne sur l'amplitude globale de la diffusion.**
- **Aucune information sur la direction.**

Les coefficients c_l, c_p et c_s

- **Tenseur = somme d'un tenseur sphérique, plat et linéaire :**

D = c_l * + c_p * + c_s *

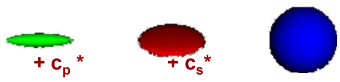

$$c_s = 3\frac{\lambda_3}{\lambda_1+\lambda_2+\lambda_3}$$
$$c_p = 2\frac{\lambda_2-\lambda_3}{\lambda_1+\lambda_2+\lambda_3}$$
$$c_l = \frac{\lambda_1-\lambda_2}{\lambda_1+\lambda_2+\lambda_3}$$
$$c_s + c_p + c_l = 1$$

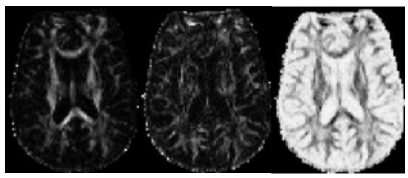

L'Anisotropie fractionnelle

- **Fractional Anisotropy (FA) = variance normalisée des valeurs propres (FA entre 0 et 1).**

$$\mathrm{FA} = \sqrt{\frac{3}{2}\left(\frac{\sum_{i=1}^{3}(\lambda_i-\lambda)^2}{\sum_{i=1}^{3}\lambda_i^2}\right)}$$
$$\text{avec } \lambda = \frac{\sum_{i=1}^{3}\lambda_i}{3}$$

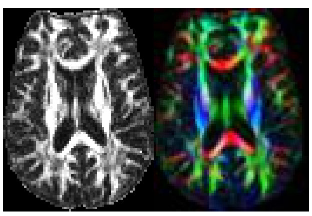

- **FA élevée : régions anisotropes = fibres.**
- **FA = 0 : regions isotropes.**

Content

Diffusion Tensor Imaging

Covariance of the Brownian motion of water
-> Architecture of axonal fibers

Very noisy data

- Tensor image processing
  - Robust estimation
  - Filtering, regularization
  - Interpolation / extrapolation
- Information extraction (fibers)

Symmetric positive definite matrices

- Convex operations are stable
  - mean, interpolation
- More complex operations are not
  - PDEs, gradient descent…

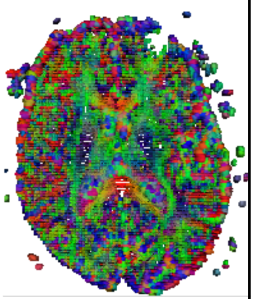

Diffusion Tensor Filed
(slice of a 3D volume)

Intrinsic computing on Manifold-valued images?

25

Probabilités et statistiques simples

Objets géométriques :

- Primitives : points orientes, repères…
- Transformations : rigides, rotations

➔ Variétés différentielles

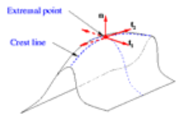

Mesure : vecteur aleatoire x de densite $p_{\mathbf{x}}(z)$

Approximation : $\mathbf{x} \sim (\bar{\mathrm{x}}, \boldsymbol{\Sigma}_{\mathbf{xx}})$

Propagation : $\mathbf{y} = h(\mathbf{x}) \sim \left(h(\bar{\mathrm{x}}),\ \frac{\partial h}{\partial \mathrm{x}}.\boldsymbol{\Sigma}_{\mathbf{xx}}.\frac{\partial h}{\partial \mathrm{x}}^{\mathrm{T}} \right)$

Modèle de bruit : additif, gaussien...

Distance statistique : Mahalanobis et χ^2

26

Quelques problèmes avec la géométrie

Moyenne de rotations 3D : Définition intrinsèque (indep. de la carte)

$$\underline{\mathbf{R}} = \frac{1}{n}\sum_i \mathbf{R}_i \qquad \underline{q} = \frac{1}{n}\sum_i q_i \qquad \underline{r} = \frac{1}{n}\sum_i r_i$$

Bruit IID sur les rotations : invariance par un groupe de transfo.

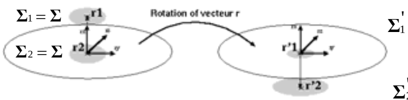

$\Sigma'_1 = \frac{8}{\pi^2}\Sigma$

$\Sigma'_2 = \frac{\pi^2}{8}\Sigma$

$$\Sigma = \sigma^2 \begin{bmatrix} 0 & 0 & 0 \\ 0 & 1 & 0 \\ 0 & 0 & 1 \end{bmatrix}$$

27

Riemannian Manifolds: geometrical tools

Riemannian metric :

- Dot product on tangent space
- Speed, length of a curve
- Distance and geodesics
  - Closed form for simple metrics/manifolds
  - Optimization for more complex

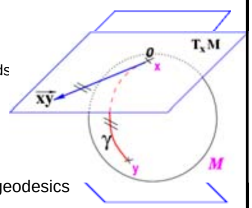

Exponential chart (Normal coord. syst.) :

- Development in tangent space along geodesics
- Geodesics = straight lines
- Distance = Euclidean
- Star shape domain limited by the cut-locus
- Covers all the manifold if **geodesically complete**

28

Computing on Riemannian manifolds

Operation	Euclidean space	Riemannian manifold
Subtraction	$\overrightarrow{xy} = y - x$	$\overrightarrow{xy} = \log_x(y)$
Addition	$y = x + \overrightarrow{xy}$	$y = \exp_x(\overrightarrow{xy})$
Distance	$dist(x, y) = \lVert y - x \rVert$	$dist(x, y) = \lVert \overrightarrow{xy} \rVert_x$
Gradient descent	$\Sigma_{t+\varepsilon} = \Sigma_t - \varepsilon \nabla C(\Sigma_t)$	$\Sigma_{t+\varepsilon} = \exp_{\Sigma_t}(-\varepsilon \nabla C(\Sigma_t))$

29

Computing on manifolds: a summary

The Riemannian metric easily gives

- Intrinsic measure and probability density functions
- Expectation of a function from M into R (variance, entropy)

Integral or sum in M: minimize an intrinsic functional

- Fréchet / Karcher mean: minimize the variance
- Filtering, convolution: weighted means
- Gaussian distribution: maximize the conditional entropy

The exponential chart corrects for the curvature at the reference point

- Gradient descent: geodesic walking
- Covariance and higher order moments
- Laplace Beltrami for free

[Pennec, NSIP'99, JMIV 2006, Pennec et al, IJCV 66(1) 2006, Arsigny, PhD 2006]

30

Statistical Analysis of the Scoliotic Spine

[J. Boisvert, X. Pennec, N. Ayache, H. Labelle, F. Cheriet,, ISBI'06]

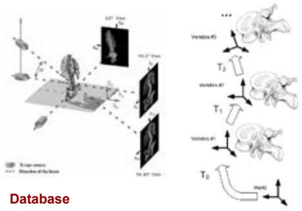

Database

- 307 Scoliotic patients from the Montreal's Sainte-Justine Hospital.
- 3D Geometry from multi-planar X-rays

Mean

- Main translation variability is axial (growth?)
- Main rotation var. around anterior-posterior axis

PCA of the Covariance

- 4 first variation modes have clinical meaning

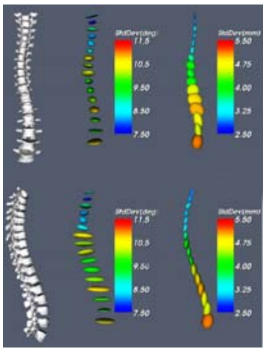

Statistical Analysis of the Scoliotic Spine

- Mode 1: King's class I or III
- Mode 2: King's class I, II, III
- Mode 3: King's class IV + V
- Mode 4: King's class V (+II)

Content

A Riemannian Framework on tensors

Affine-invariant Metric (Curved space – Hadamard)

- Action of the linear group GLn $A * \Sigma = A \Sigma . A^T$
- Dot product $\langle V \mid W \rangle_\Sigma = \langle AVA^T \mid AWA^T \rangle_{A\Sigma A^T} = \langle \Sigma^{-1/2} V \Sigma^{-1/2} \mid \Sigma^{-1/2} W \Sigma^{-1/2} \rangle_{Id}$
- Geodesics: $\Gamma_{Id,W}(t) = \exp(tW)$
- Exponential map:

$$\exp_\Sigma(\overrightarrow{\Sigma\Psi}) = \Sigma^{1/2} \exp(\Sigma^{-1/2} . \overrightarrow{\Sigma\Psi} . \Sigma^{-1/2}) \Sigma^{1/2}$$

- Log map:

$$\overrightarrow{\Sigma\Psi} = \log_\Sigma(\Psi) = \Sigma^{1/2} \log(\Sigma^{-1/2} . \Psi . \Sigma^{-1/2}) \Sigma^{1/2}$$

- Distance

$$\boxed{\mathrm{dist}(\Sigma, \Psi)^2 = \langle \overrightarrow{\Sigma\Psi} \mid \overrightarrow{\Sigma\Psi} \rangle_\Sigma = \left\| \log(\Sigma^{-1/2} . \Psi . \Sigma^{-1/2}) \right\|_{L_2}^2}$$

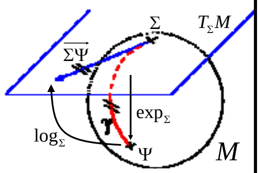

[Pennec, Fillard, Ayache, IJCV 66(1), 2006, Lenglet JMIV'06, etc]

Tensor interpolation

Geodesic walking in 1D $\Sigma(t) = \exp_{\Sigma_1}(t \overrightarrow{\Sigma_1 \Sigma_2})$

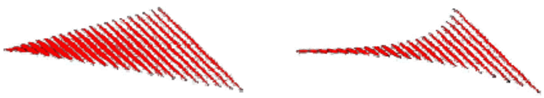

Weighted mean in general $\Sigma(x) = \min_\Sigma \sum w_i(x)\ dist(\Sigma, \Sigma_i)^2$

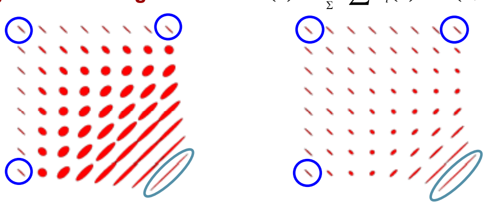

Gaussian filtering: Gaussian weighted mean

$$\Sigma(x) = \min \sum_{i=1}^{n} G_\sigma(x - x_i)\ dist(\Sigma, \Sigma_i)^2$$

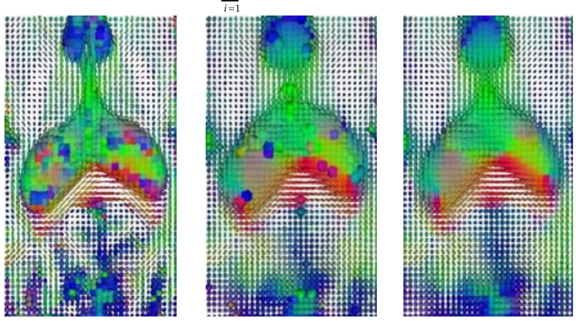

Raw — Coefficients σ=2 — Riemann σ=2

PDE for filtering and diffusion

Harmonic regularization $C(\Sigma) = \int_{\Omega} \|\nabla \Sigma(x)\|^2_{\Sigma(x)} dx$

- Gradient = manifold Laplacian

$$\Delta \Sigma(x) = \sum_i \partial_i^2 \Sigma - \sum_i (\partial_i \Sigma) \Sigma^{(-1)} (\partial_i \Sigma) = \sum_u \frac{\overrightarrow{\Sigma(x)\Sigma(x+u)}}{\|u\|^2} + O\left(\|u\|^2\right)$$

- Integration through geodesic marching

$$\Sigma_{t+1}(x) = \exp_{\Sigma_t(x)}\left(-\varepsilon \nabla C(\Sigma)(x)\right)$$

Anisotropic regularization

- Perona-Malik 90 / Gerig 92
- Phi functions formalism [Odyssee / Deriche]

37

Anisotropic filtering

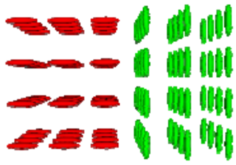
Initial

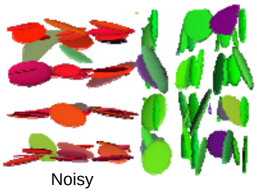
Noisy

Recovered
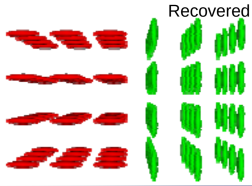

38

Anisotropic filtering

$$\Delta_w \Sigma(x) = \sum_u w\left(\partial_u \Sigma(x)\right) \Delta_u \Sigma(x) \quad \text{with} \quad w(t) = \exp(-t^2/\kappa^2)$$

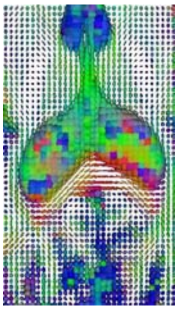
Raw

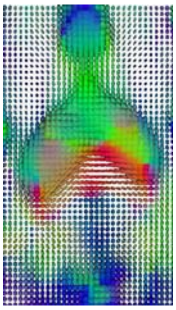
Riemann Gaussian

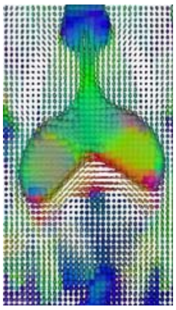
Riemann anisotropic

39

Content

Recalage iconique et deformable (rappel)

Imagerie du tenseur de diffusion

Tensor Computing

- Statistical computing on manifolds
- Interpolation, filtering, diffusion PDEs
- Other metrics
- Applications in Diffusion tensor imaging

Computational Anatomy

Conclusion

40

Log Euclidean Metric on Tensors

Exp/Log: global diffeomorphism Tensors/sym. matrices

- Vector space structure carried from the tangent space to the manifold
  - Log. product $\Sigma_1 \otimes \Sigma_2 \equiv \exp\left(\log(\Sigma_1) + \log(\Sigma_2)\right)$
  - Log scalar product $\alpha \bullet \Sigma \equiv \exp\left(\alpha \log(\Sigma)\right) = \Sigma^{\alpha}$
  - Bi-invariant metric $\boxed{dist\left(\Sigma_1, \Sigma_2\right)^2 \equiv \left\|\log(\Sigma_1) - \log(\Sigma_2)\right\|^2}$

Properties

- Invariance by the action of similarity transformations only
- Very simple algorithmic framework

[Arsigny, Fillard, Pennec, Ayache, MICCAI 2005, T1, p.115-122]

41

Riemannian Frameworks on tensors

Affine-invariant Metric (Curved space – Hadamard)

- Dot product $\langle V \mid W \rangle_{\Sigma} = \langle AVA^T \mid AWA^T \rangle_{A\Sigma A^T} = \langle \Sigma^{-1/2} V \Sigma^{-1/2} \mid \Sigma^{-1/2} W \Sigma^{-1/2} \rangle_{Id}$
- Geodesics $\exp_{\Sigma}(\overrightarrow{\Sigma\Psi}) = \Sigma^{1/2} \exp(\Sigma^{-1/2}.\overrightarrow{\Sigma\Psi}.\Sigma^{-1/2}) \Sigma^{1/2}$
- Distance $\boxed{\mathrm{dist}(\Sigma, \Psi)^2 = \langle \overrightarrow{\Sigma\Psi} \mid \overrightarrow{\Sigma\Psi} \rangle_{\Sigma} = \left\|\log(\Sigma^{-1/2}.\Psi.\Sigma^{-1/2})\right\|^2_{L_2}}$

[Pennec, Fillard, Ayache, IJCV 66(1), 2006, Lenglet JMIV'06, etc]

Log-Euclidean similarity invariant metric (vector space)

- Transport Euclidean structure through matrix exponential
- Dot product $\langle V \mid W \rangle_{\Sigma} = \langle \partial_V \log(\Sigma) \mid \partial_W \log(\Sigma) \rangle_{Id}$
- Geodesics $\exp_{\Sigma}(\overrightarrow{\Sigma\Psi}) = \exp(\log(\Sigma) + \partial_{\overrightarrow{\Sigma\Psi}} \log(\Sigma))$
- Distance $\boxed{\mathrm{dist}\left(\Sigma_1, \Sigma_2\right)^2 \equiv \left\|\log(\Sigma_1) - \log(\Sigma_2)\right\|^2}$

[Arsigny, Pennec, Fillard, Ayache, SIAM'06, MRM'06]

42

Log Euclidean vs Affine invariant

- Both means are geometric (vs arithmetic for Euclidean)
- Log Euclidean slightly more anisotropic
- Speedup ratio: 7 (aniso. filtering) to >50 (interp.)

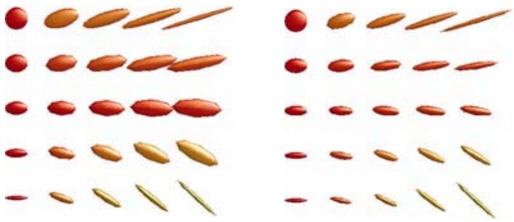

Euclidean — Affine invariant / Log-Euclidean

[Arsigny, Fillard, Pennec, Ayache, MICCAI 2005, MRM'06]

43

Log Euclidean vs Affine invariant

Real DTI images: anisotropic filtering

- Both means are geometric (vs arithmetic for Euclidean)
- Log Euclidean slightly more anisotropic
  but the difference is not significant
- Speedup ratio: 7 (aniso. filtering) to >50 (interp.)

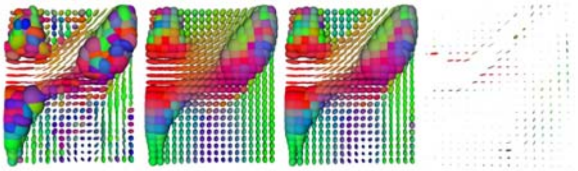

Original — Euclidean — Log-Euclidean — Diff. LE/affine (x100)

[Arsigny, Fillard, Pennec, Ayache, MICCAI 2005, MRM'06]

44

Regularization of the Structure Tensor

Structure tensor (guide for diffusion) $\Sigma_\sigma(x) = G_\sigma * \left(\nabla I \, \nabla I^t\right)$

Original

SNR 10% added

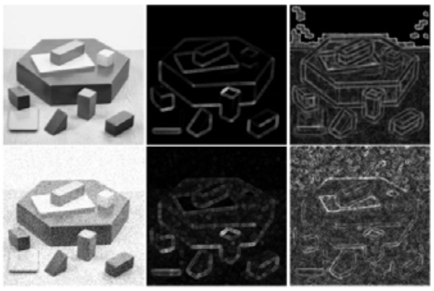

Image — Euclidean grad — Riemannian grad

[Fillard, Arsigny, Ayache, Pennec, DSSCV'05]

45

Regularization of the Structure Tensor

Anisotropic diffusion of the Euclidean grad is unstable!

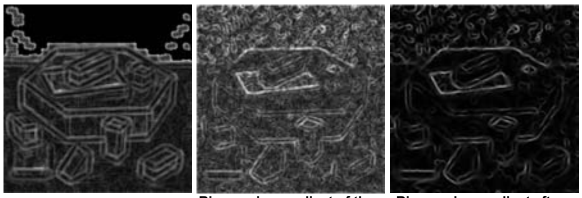

Riemannian gradient — Riemannian gradient of the noisy image — Riemannian gradient after filtering

Filtering parameters: κ=0.02, dt=0.1, 500 iterations.

But Riemannian anisotropic diffusion preserve small noise

46

Geodesic shooting in tensors spaces

A null eigenvalue is physically plausible: it is a perfect straight edge

Need to change the metric?

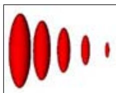

Undefined (non positive)

Euclidean metric

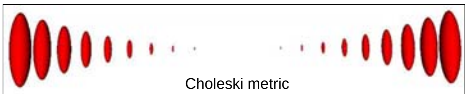

Choleski metric

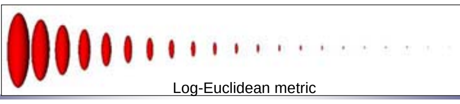

Log-Euclidean metric

47

Content

Recalage iconique et deformable (rappel)

Imagerie du tenseur de diffusion

Tensor Computing

- Interpolation, filtering, diffusion PDEs
- Other metrics
- Applications in Diffusion tensor imaging

Computational Anatomy

Conclusion

48

ML and MAP estimation from DWI with Rician noise

$$C(\Sigma)=\int \sum_i \left(S_i - S_0 \exp\left(-b\, \mathbf{g}_i^T \Sigma(x)\, \mathbf{g}_i\right)\right)^2 + \Phi\left(\|\nabla\Sigma(x)\|^2_{\Sigma(x)}\right)$$

Clinical DTI of the spinal cord

FA

Estimated tensors

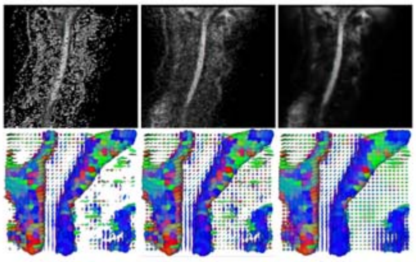

Standard ML Rician MAP Rician

[Fillard, Arsigny, Pennec, Ayache, ISBI 2005]

Joint Estimation and regularization from DWI

Clinical DTI of the spinal cord: fiber tracking

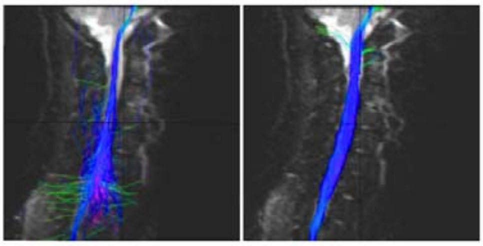

Standard MAP Rician

[Fillard, Arsigny, Pennec, Ayache, ISBI 2005]

Impact on fibers tracking

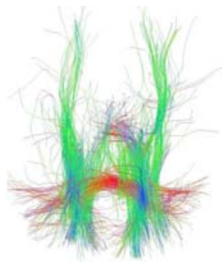

Euclidean interpolation

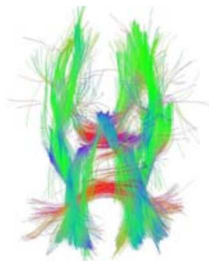

Riemannian interpolation + anisotropic filtering

[Fillard, Toussaint et al, MedINRIA: DTI Processing and Visualization Software, 2006]

From images to anatomy

- Classify fibers into tracts (anatomo-functional architecture)?
- Compare fiber tracts between subjects?

Impact on fibers tracking

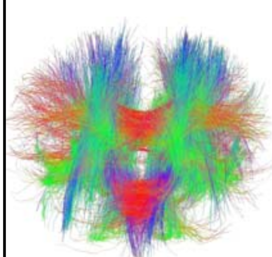

Euclidean interpolation

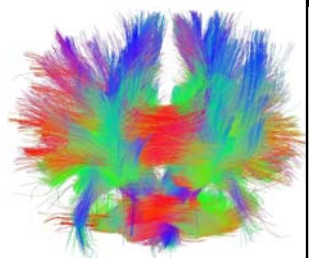

Riemannian interpolation + anisotropic filtering

[Fillard, Toussaint et al, MedINRIA: DTI Processing and Visualization Software, 2006]

From images to anatomy

- Classify fibers into tracts (anatomo-functional architecture)?
- Compare fiber tracts between subjects?

Quelques résultats

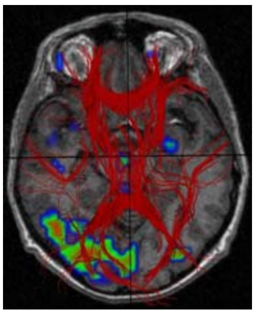

T1 + carte d'activation + fibres

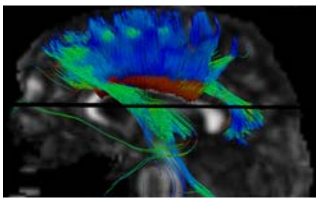

corps calleux + cingulum

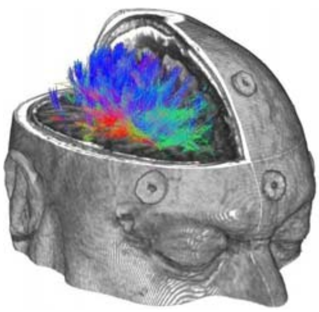

Fibres + T1 en volume rendering

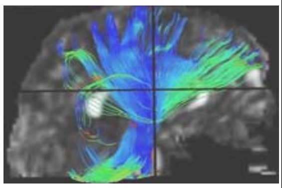

faisceau corticospinal et couronne rayonnante

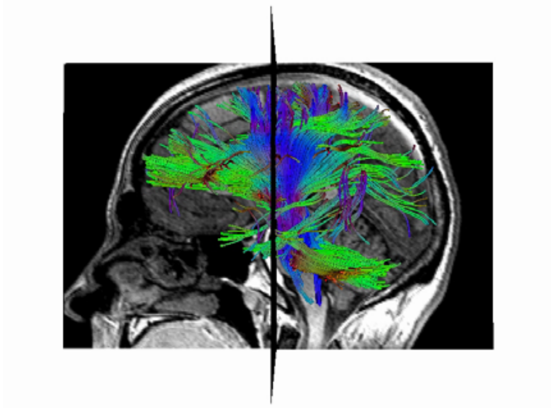

Towards a Statistical Atlas of Cardiac Fiber Structure

[J.M. Peyrat, et al., MICCAI'06, TMI 26(11), 2007]

Database
- 7 canine hearts from JHU
- Anatomical MRI and DTI

Method
- Normalization based on aMRIs
- Log-Euclidean statistics of Tensors

Norm covariance

Eigenvalues covariance (1^{st}, 2^{nd}, 3^{rd})

Eigenvectors orientation covariance (around 1st, 2nd, 3rd)

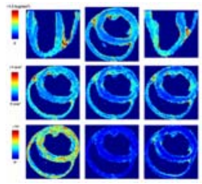

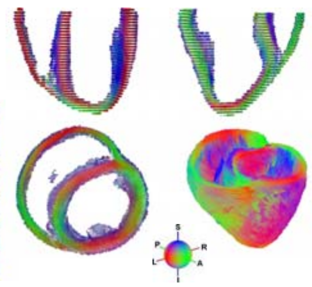

Content

Recalage iconique et deformable (rappel)

Imagerie du tenseur de diffusion

Tensor Computing

Computational Anatomy
- Morphometry of sulcal lines on the brain
- Statistics of deformations for non-linear registration

Conclusion

Anatomy

Science that studies the structure and the relationship in space of different organs and tissues in living systems [Hachette Dictionary]

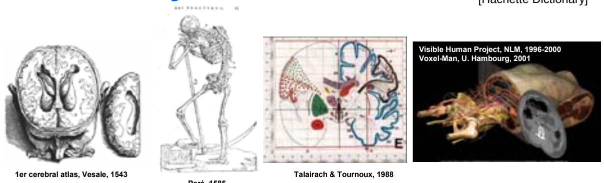

1er cerebral atlas, Vesale, 1543

Paré, 1585

Talairach & Tournoux, 1988

Antiquity
• Animal models
• Philosophical physiology

Renaissance:
• Dissection, surgery
• Descriptive anatomy

17-20e century:
• Anatomo-physiology
• Microscopy, histology

1990-2000:
• Explosion of imaging
• Computer atlases
• Brain decade

Galien (131-201) | Vésale (1514-1564) Paré (1509-1590) | Sylvius (1614-1672) Willis (1621-1675) | Gall (1758-1828) : *Phrenology* Talairach (1911-2007)

Revolution of observation means (1988-2007) :
- From dissection to in-vivo in-situ imaging

The revolution of medical imaging

In vivo observation of living systems
- A large number of modalities to image anatomy and function
  - Growing spatial resolution (molecules to whole body)
  - Multiple temporal scales

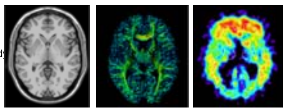

brain

Non invasive observations
- Emergence of large databases
- **From representative individual to population**

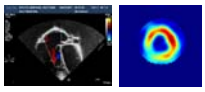

heart

Extract and structure information
- 50 to 150 MB for a clinical MRI
- Computer analysis is necessary
- **From descriptive atlases to interactive and generative models** (simulation)
  - MNI 305 (1993), ICBM 152 (2001), Brain web (1999)
  - Bone Morphing® (Fleute et al, 2001)

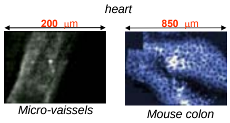

Micro-vaissels   *Mouse colon*

Computational Anatomy

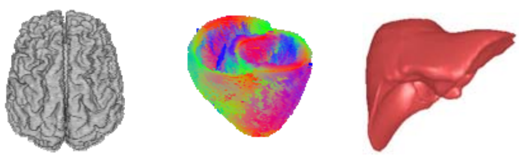

***Computational Anatomy, an emerging discipline*, P. Thompson, M. Miller, NeuroImage special issue 2004**

***Mathematical Foundations of Computational Anatomy*, X. Pennec, S. Joshi, MICCAI workshop, 2006**

Modeling and Analysis of the Human Anatomy
- Estimate representative / average organ anatomies
- Model organ development across time
- Establish normal variability
- To detect and classify of pathologies from structural deviations
- To adapt generic (atlas-based) to patients-specific models

⇨Statistical analysis on (and of) manifolds

Structural variability of the Cortex

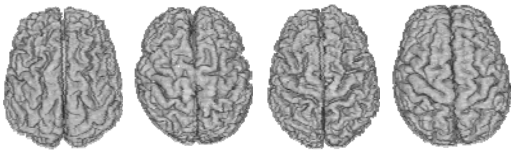

Hierarchy of anatomical manifolds

- Landmarks [0D]: AC, PC (Talairach)
- Curves [1D]: crest lines, sulcal lines
- Surfaces [2D]: cortex, sulcal ribbons
- Images [3D functions]: VBM
- Transformations: rigid, multi-affine, diffeomorphisms [TBM]

62

Morphometry of the Cortex from Sucal Lines

Associated team Brain-Atlas (2001-2006)

LONI

- LONI (UCLA) : P. Thompson et al.
- ASCLEPIOS (INRIA): V. Arsigny, N. Ayache, P. Fillard, X. Pennec

Neuroanatomical reference:

- 72 sulcal lines manually extracted and labeled
- 700 subjects

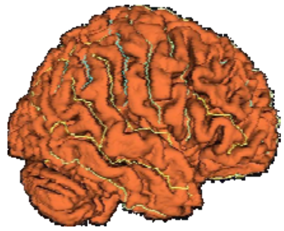

Alternative

- Automatic extraction

JF. Mangin, D. Rivière, 2003, SHFJ-CEA

63

Morphometry of the Cortex from Sucal Lines

Computation of the mean sulci: Alternate minimization of global variance

- Dynamic programming to match the mean to instances
- Gradient descent to compute the mean curve position

Extraction of the covariance tensors

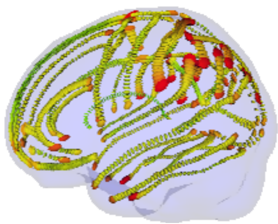

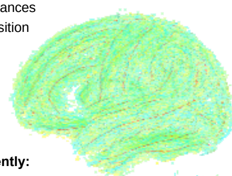

Currently:

80 instances of 72 sulci

About 1250 tensors

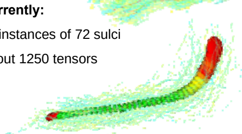

Covariance Tensors along Sylvius Fissure

Collaborative work between Asclepios (INRIA) Vand LONI (UCLA) P. Thompson
[Fillard et al IPMI05, LNCS 3565:27-38, NeuroImage 34(2):639-650, January 2007]

64

Compressed Tensor Representation

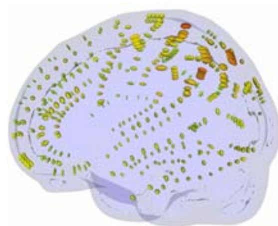

Representative Tensors (250)

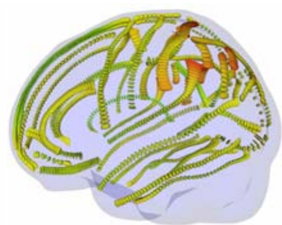

Reconstructed Tensors (1250)
(Riemannian Interpolation)

65

Extrapolation by Diffusion

$$C(\Sigma) = \frac{1}{2}\int_{\Omega}\sum_{i=1}^{n} G_{\sigma}(x-x_i)\,dist(\Sigma(x),\Sigma_i)^2\,dx + \frac{\lambda}{2}\int_{\Omega}\left\|\nabla\Sigma(x)\right\|^2_{\Sigma(x)}$$

$$\nabla C(\Sigma)(x) = -\sum_{i=1}^{n} G_{\sigma}(x-x_i)\overrightarrow{\Sigma(x)\Sigma_i} - \lambda(\Delta\Sigma)(x)$$

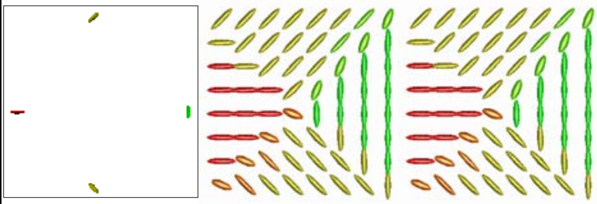

Original tensors　　Diffusion λ=0.01　　Diffusion $\lambda=\infty$

67

Full Brain extrapolation of the variability

$$C(\Sigma) = \frac{1}{2}\int_{\Omega}\sum_{i=1}^{n} G_{\sigma}(x-x_i)\,dist(\Sigma(x),\Sigma_i)^2\,dx + \frac{\lambda}{2}\int_{\Omega}\left\|\nabla\Sigma\right\|^2_{\Sigma(x)}$$

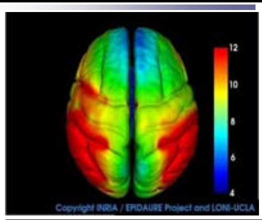

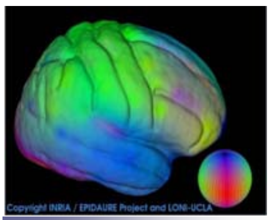

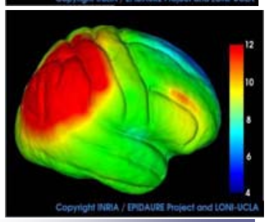

68

Comparison with cortical surface variability

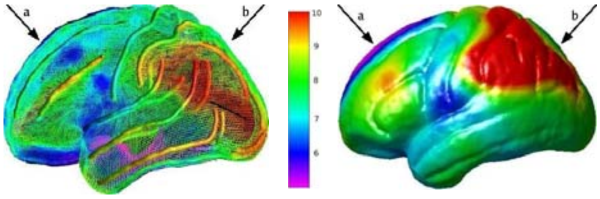

P. Thompson at al, HMIP, 2000
Average of 15 normal controls by non-linear registration of surfaces

P. Fillard et al, IPMI 05
Extrapolation of our model estimated from 98 subjects with 72 sulci.

Consistent low variability in phylogenetical older areas
- (a) superior frontal gyrus

Consistent high variability in highly specialized and lateralized areas
- (b) temporo-parietal cortex

Asymmetry Measures

$$dist(\Sigma,\Sigma')^2 = \left\langle \overrightarrow{\Sigma\Sigma'} \mid \overrightarrow{\Sigma\Sigma'} \right\rangle_\Sigma = \left\| \log(\Sigma^{-1/2}.\Sigma'.\Sigma^{-1/2}) \right\|_{L_2}^2$$

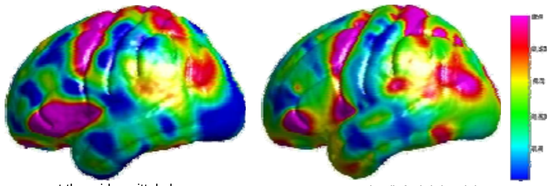

w.r.t the mid-sagittal plane.

w.r.t opposite (left-right) sulci

Greatest asymmetry	Lowest asymmetry
Broca's speech area and Wernicke's language comprehension area	Primary sensorimotor areas

Symmetry of the variability between groups

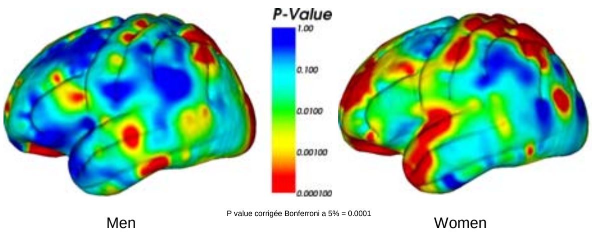

Men

Women

[Fillard, Pennec,Thompson, Thompson, Evaluating Brain Anatomical Correlations via Canonical Correlation Analysis of Sulcal Lines, MICCAI Workshop on stat. Atlases, 2007]

Local and distant structural correlation

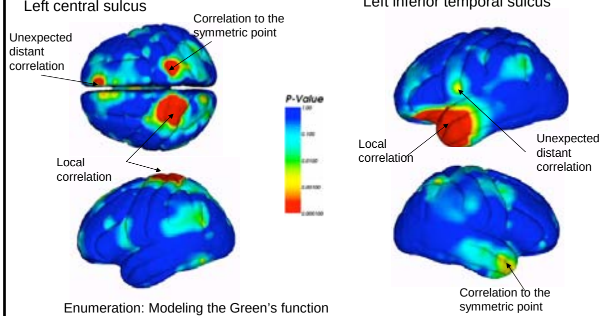

Enumeration: Modeling the Green's function

[Fillard, Pennec,Thompson, Thompson, Evaluating Brain Anatomical Correlations via Canonical Correlation Analysis of Sulcal Lines, MICCAI Workshop on stat. Atlases, 2007]

An alternative approach with diffeomorphisms

[S, Durrleman, X. Pennec, A. Trouvé, N. Ayache, MICCAI 2007]

Does the method influence results?
- Matching, then extrapolation [Fillard, NeuroImage 34(2) 2007]
- Extrapolation of speed vectors and trajectory integration

Method
- Global space diffeomorphism (integration of time varying vector fields) [Trouve, Younes, Miller, etc]
- Distance between lines using currents [J. Glaunès, M. Vaillant: IPMI 2005]

Advantages
- Generative model of deformations
- Retrieve some tangential deformation component.

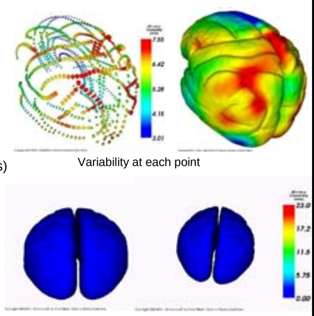

Variability at each point

Global variability (2 PGA modes)

Content

Recalage iconique et deformable (rappel)

Imagerie du tenseur de diffusion

Tensor Computing

Computational Anatomy
- Morphometry of sulcal lines on the brain
- Statistics of deformations for non-linear registration

Conclusion

Use of the variability information?

Learning / modeling phase (anatomy / neurosciences)

- Goal: analyze and understand the population variability
- Fact: Methods have different assumptions
  - Similar results at some locations, different results at other places
  - Each method is based on partial observations
  - Each method is biased by its assumptions
- → Vary assumptions / data, and discover "truth" by consensus

Personalization of atlases (use in a clinical / medical workflow)

- Anatomical prior to compensate for incomplete / noisy / abnormal (pathological) observations.
- Use variability statistics as a regularizer to robustify registration?

One example use of variability information: better constrain the atlas to subject registration

- Deform the atlas anatomy (without tumor) towards the patient one
- Segment the structures of interest in the patient image
- Minimize irradiation in areas at risk.

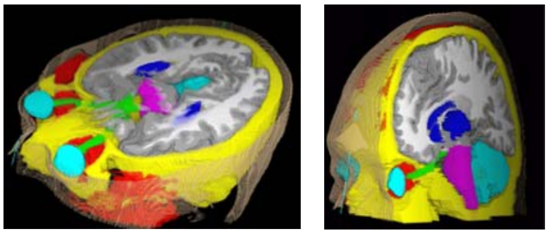

[Commowick, et al, MICCAI 2005]

Introducing local variability and pathologies in non-linear registration

$$E(T) \quad = \quad E_{sim}(I, J(T)) \ + \ \lambda . E_{reg}(T)$$

- Non stationary regularization: anatomical prior on the deformability
- Non stationary image similarity / regularization tradeoff: takes pathologies into account

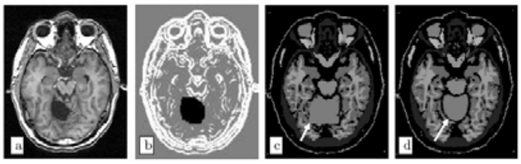

Patient Stiffness field Atlas to patient With pathology

[Runa. Stefanescu et al, PPL 14(2), 2004 & Med. Image Analysis 8(3), 2003]

Regularization in dense non-linear registration

Physically based regularizations

- Elastic [Bajcsy 89]
- Fluid [Christensen TMI 97]
- Right-invariant distance [LDDMM, Beg IJCV 05]

Efficient regularization methods

- Gaussian filtering [Thirion Media 98, Modersitzki 2004]
- Isotropic but non stationary [Lester IPMI'99]
- Towards anisotropic non stationary regularization [Stefanescu MedIA 2004]

Observation:

- **Inter-subject**: no regularization model is more justified than others
- Idea: learning statistically the variability from a population [Thompson 2000, Rueckert TMI 2003, Fillard IPMI 2005]

Statistics on the deformation field

- Objective: planning of conformal brain radiotherapy (O. Commowick, Dosisoft)
- 30 patients, 2 to 5 time points (P-Y Bondiau, MD, CAL, Nice)

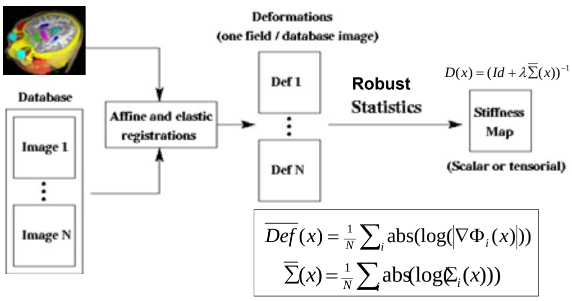

$$\overline{Def}(x) = \tfrac{1}{N}\sum_i \mathrm{abs}(\log(|\nabla\Phi_i(x)|))$$

$$\overline{\Sigma}(x) = \tfrac{1}{N}\sum_i \mathrm{abs}(\log(\Sigma_i(x)))$$

[Commowick, et al, MICCAI 2005, T2, p. 927-931]

Introducing deformation statistics into RUNA

RUNA [R. Stefanescu et al, Med. Image Analysis 8(3), 2004]

- non linear-registration with non-stationary regularization
- Scalar or tensor stiffness map $D(x) = (Id + \lambda\overline{\Sigma}(x))^{-1}$

Heuristic RUNA stiffness **Scalar statistical stiffness** **Tensor stat. stiffness (FA)**

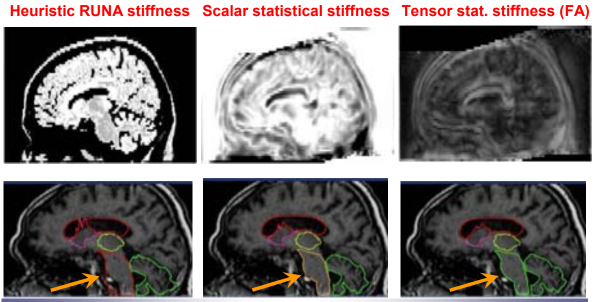

Riemannian elasticity for Non-linear elastic regularization

Regularization

- Local deformation measure: Cauchy Green strain tensor $\Sigma = \nabla\Phi^t.\nabla\Phi$
  - Id for local rotations, small for local contractions, Large for local expansions
- St Venant Kirchoff elastic energy $\mathrm{Reg}(\Phi) = \int \mu\, \mathrm{Tr}\left((\Sigma - I)^2\right) + \frac{\lambda}{2} \mathrm{Tr}(\Sigma - I)^2$
  - Elasticity is not symmetric
  - Statistics are not easy to include

Statistics on the Henky strain tensor: learning the deformation metric

- Idea: Euclidean -> log-Euclidean $\mathrm{Tr}\left((\Sigma - I)^2\right) \rightarrow \mathrm{dist}_{LE}(\Sigma, I)^2 = \|\log(\Sigma)\|^2$
  - Mean, covariance, Mahalanobis computed in Log-space
- Riemannian Elasticity $\mathrm{Reg}(\Phi) = \int \mathrm{Vect}\left(\log(\Sigma) - \overline{W}\right)^T.\mathrm{Cov}^{-1}.\mathrm{Vect}\left(\log(\Sigma) - \overline{W}\right)$
  - Isotropic case: $\mathrm{Reg}_{\mathrm{iso}}(\Phi) = \int \mu\, \mathrm{Tr}\left(\log(\Sigma)^2\right) + \frac{\lambda}{2} \mathrm{Tr}\left(\log(\Sigma)\right)^2$
- Locally consistent measure of deformation statistics / regularization criterion

[Pennec, et al, MICCAI 2005]

Isotropic Riemannian Elasticity Results

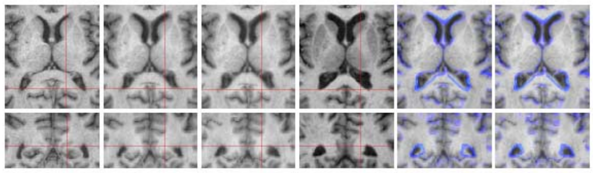

Source image | Elastic result | Riemann res. | Target image | Elast.+target | Riem.+target

Roi 186x124x216 voxels, $\lambda=\mu=0.2$, 12 PC 2Gh.

- Larger computation times 3h vs 1h
- Slightly larger and better deformation of the right ventricle
  without any statistical information yet…

[Pennec, et al, MICCAI 2005, T2, p.943-950]

Content

Recalage iconique et deformable (rappel)

Imagerie du tenseur de diffusion

Tensor Computing

Computational Anatomy

Conclusion

Statistics on geometrical objects

A consistent framework with important applications in

- Medical Image Analysis (registration evaluation, DTI)
- Building models of living systems (spine, brain, heart…)

Is the Riemannian metric the minimal structure?

- No bi-invariant metric but bi-invariant means on Lie groups [V. Arsigny]
  Change the Riemannian metric for the symmetric Cartan connection?

Computational framework for infinite dimensional manifolds

- Curves and surfaces: statistics on currents?
- Efficient framework for some spaces of diffeomorphisms?

How to chose or estimate the metric?

- Invariance, reacheability of boundaries, learning the metric
- Families of anatomical deformation metrics (models of the Green's function)

Challenges of Computational Anatomy

Build models from multiple sources

- Curves, surfaces [cortex, sulcal ribbons]
- Volume variability [Voxel/Tensor Based Morphometry, Riemannian elasticity]
- Diffusion tensor imaging [fibers, tracts, atlas]

Compare and combine statistics on anatomical manifolds

- Each method is biased by its assumptions (fewer data than unknowns)
- Validate methods and models by consensus

Asclepios (INRIA), Visages (IRISA),
Neurospin (CEA + INRIA),
LENA (CNRS-CHUPS),
CMLA (ENS), LSIS (CNRS).

From modeling to personalized medicine

- Topological changes
- Evolution: growth, pathologies
- Couple statistical learning / modeling and
  use of models as prior for inter-subject registration / segmentation

Acknowledgements

Image guided therapy

- Brain surgery (Roboscope): A. Roche and P. Cathier
- Dental implantology: S. Granger, AREALL
- Liver puncture guidance: S. Nicolau and L. Soler, IRCAD
- Mosaicing confocal microscopic images: T. Vercauteren, MKT

Brain imaging

- Geometry and statistics for fMRI analysis: G. Flandin, J.-B. Poline, CEA
- Inter-subject non-linear registration: P. Cathier, R. Stefanescu, O. Commowick

Computational anatomy

- Associated team Brain Atlas with LONI: P. Thompson, P. Fillard, V. Arsigny
- Growth and variability: S. Durrleman
- Spine shape: J. Boisvert, F. Cheriet, Ste Justine Hospital, Montreal.
- ACI Agir / Grid computing: T. Glatard and J. Montagnat, I3S.

Epidaure / Asclepios Team

- N. Ayache, G. Malandain, H. Delingette
- … and all the current and former team members.